Characterization of a Variable Friction Damper on Drum Brake Technology

Liang Cao[1], Austin Downey[1], Simon Laflamme[1], Douglas Taylor[2], and James Ricles[3]

Abstract

The authors have recently proposed a novel variable friction damping device for semi-active control of civil structures. The damping mechanism is based on a duo-servo drum brake technology, and leverages its self-energizing mechanism to produce large damping forces using low energy input. Compared to other semi-active damping systems, the proposed device combines the advantages of cost-effectiveness, high theoretical damping performance, mechanical robustness, and technological simplicity. Here, a prototype is constructed by altering an existing duo-servo automobile brake. The dynamic behavior of the prototype is characterized at low displacement under different velocities. Experimental verification shows that the braking technology exhibits a linear behavior in damping forces when the rotation is reversed, and that non-negligible additional rotation is required before the shoes slip on the drum brake to deliver a friction force. A three stage dynamic model is proposed. Stage 1 models the friction using the LuGre model; stage 2 models a linear stiffness found in the system when the direction reversed, and stage 3 models the rapid build up of forces linearly. Results show that the three stages model leads to a good fit of experimental data for different input forces at low displacement under different velocities.

I. INTRODUCTION

Supplemental damping has been shown to be cost-effective in reducing structural response under service and extreme loads. Such damping can be provided by passive, active, semi-active, or hybrid systems. Passive control systems are now widely accepted in the field of structural engineering. These devices do not need power to operate and are generally mechanically robust, but their performance is typically limited within a given excitation bandwidth [1]–[3]. Conversely, active control systems can cover a wide range of excitation bandwidths, but require significant power to operate and may destabilize a system [4].

An alternative is to utilize semi-active systems. These devices have gained popularity due to their enhanced controllability with respect to passive devices, low power requirement and inherent stability. Examples include variable stiffness [5], [6], variable friction [7], variable fluid [8]–[10], and variable orifice [11] devices. The authors have recently proposed a novel semi-active friction device, termed Modified Friction Device (MFD), theoretically capable of developing large damping forces using low power [12]. The MFD is based on an automobile drum brake, a mature and reliable technology. The high damping capability arises from the self-energizing mechanism of duo servo drum brakes, and the variable friction force is obtained by varying the pressure on the braking shoes. The MFD arranged in parallel with a stiffness and a viscous element mimics the dynamics of a magnetorheological damper [16]. In prior work, the promise of the MFD has been demonstrated via simulations on a full-scale structure [12].

In this paper, we experimentally investigate the dynamic behavior of the MFD. While the friction mechanism of automobile brakes is well understood in vehicle applications, the dynamics of friction at low displacements and low velocities is yet to be modeled in both forward and backward rotations. The MFD is prototyped using a duo servo drum brake due to the readily availability of the components, and characterized at low displacement under different velocities, at various pressures (force input). A three stage dynamic model is proposed to model the dynamics of the MFD in both forward and backward rotations. The model consists of a LuGre friction model to characterize the friction zone (Stage 1), and two pure stiffness regions to characterize the dynamics of the MFD once the rotation is reversed and the braking shoes are sticking to the drum (Stage 2), and the rapid build up of forces once one shoe is anchored to the pin (Stage 3). The model is validated experimentally.

The paper is organized as follows. Section II provides background on the mechanical principle of the MFD, and describes the prototype. Section III introduces the three stage dynamic model used to characterize the dynamics of the MFD. Section IV experimentally verifies the dynamic model. Section V summarizes and concludes the paper.

II. MODIFIED FRICTION DEVICE

A. Mechanical Principle

The MFD is designed to dissipate energy via frictional forces developed by the contact of braking shoes onto a drum. The eccentric location of the braking shoes with respect to the anchor pin produces a static moment term self-energizing effect, which has the potential to substantially amplify the brake actuation force [13]. Fig. 1 shows a schematic representation of the MFD describing the internal components (Fig. 1 (a)) and the diagram of forces (Fig. 1 (b)). This friction dynamics of the MFD is described in details in Ref. [14]. Briefly, the actuation force $W = pA$, where p is the actuation pressure and A the

[1]Department of Civil, Construction, and Environmental Engineering, Iowa State University, Ames, IA 50011, U.S.A
[2]Taylor Devices, North Tonawanda, NY 14120, U.S.A
[3]Department of Civil and Environmental Engineering, Lehigh University, Bethlehem, PA 18015, U.S.A

area of the actuator, acts on the braking shoes (thick blue lines in the Figure) to create normal forces N_i on shoes $i = 1, 2$, which in turn generates friction forces f_i. The total damping force $F = f_1 + f_2$ is directly related to the self-energizing effect where $F = CW$, with C being the self-energizing factor. Installed in a vertical configuration, the MFD is designed to sit on two short support legs that produce opposite forces F_{leg} to counteract the moment produced by the friction forces.

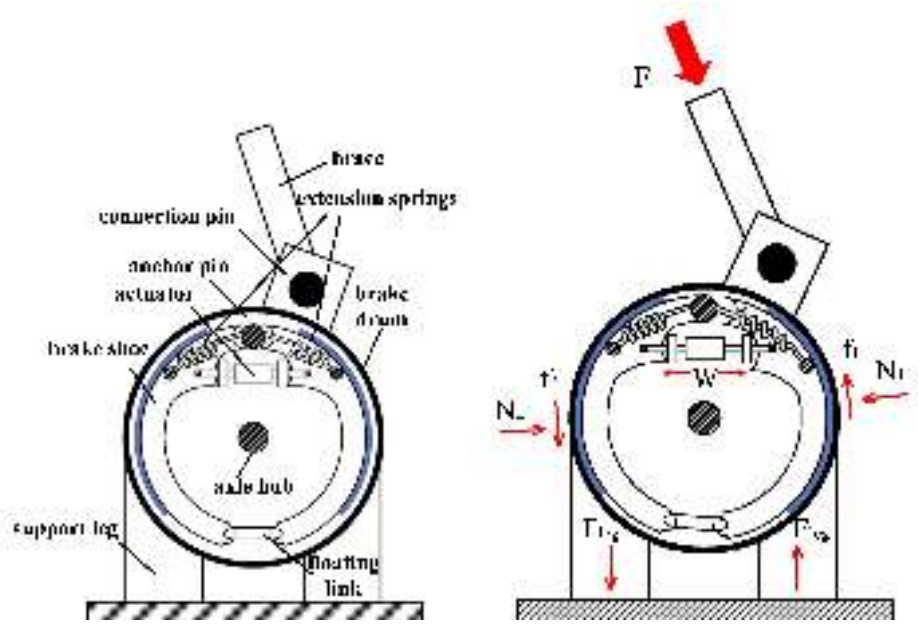

(a) (b)

Fig. 1: Schematic representation of the MFD: (a) internal components; and (b) diagram of forces

B. Prototype

A prototype of the MFD has been fabricated by modifying an automobile duo-servo drum brake due to the readily availability of the mechanical components. The braking mechanism has been modified to improve bi-directional performance by increasing the frictional contact area [15]. The drum brake has been rotated under constant hydraulic pressure during several hours in both directions to wear the lining surface. The drum has been mounted on a channel structural steel section to enable a vertical axial loading, similar to the configuration shown in Fig. 1. The force W is generated by a hand-operated hydraulic actuator.

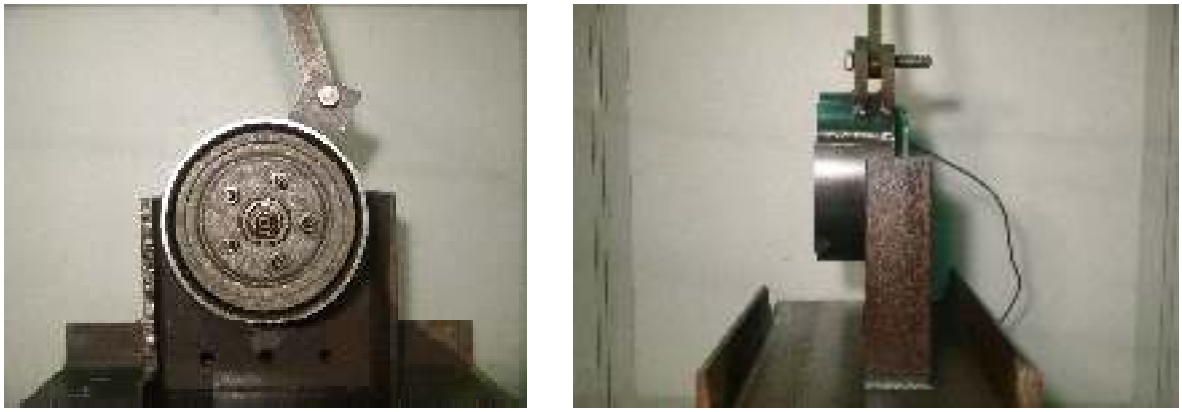

(a) (b)

Fig. 2: Prototype of the MFD: (a) front view; and (b) side view

III. DYNAMIC MODEL

The dynamics of the MFD exhibits a typical friction behavior during most of its rotation. However, when the rotation is reversed and the friction force is lost, the braking shoes will stick to the drum over a short distance, until the shoes hit the

anchor pin, after which there will be a rapid build up of the force until the brake re-enters into the typical friction dynamics.

It follows from this description that a three-stage dynamic model could be used to characterize the friction behavior of the MFD, as illustrated in Fig. 3 for a typical loop. The proposed model is as follows:

- Stage 1 (Node 1 $\longrightarrow$ Node 2) - the system is in a typical dynamic friction mode. The friction force F_1 is characterized using a LuGre friction model. This stage occurs until rotation is reversed.
- Stage 2 (Node 2 $\longrightarrow$ Node 3) - braking shoes are sticking to the drum. The linear force F_2 is characterized as being proportional to a stiffness element k_2. This stage occurs over a drum displacement d_2.
- Stage 3 (Node 3 $\longrightarrow$ Node 1) - one braking shoe is anchored at the anchor pin, and there is a rapid force build up. The force F_3 is characterized as being proportional to a stiffness element k_3. This stage occurs over a drum displacement d_3.

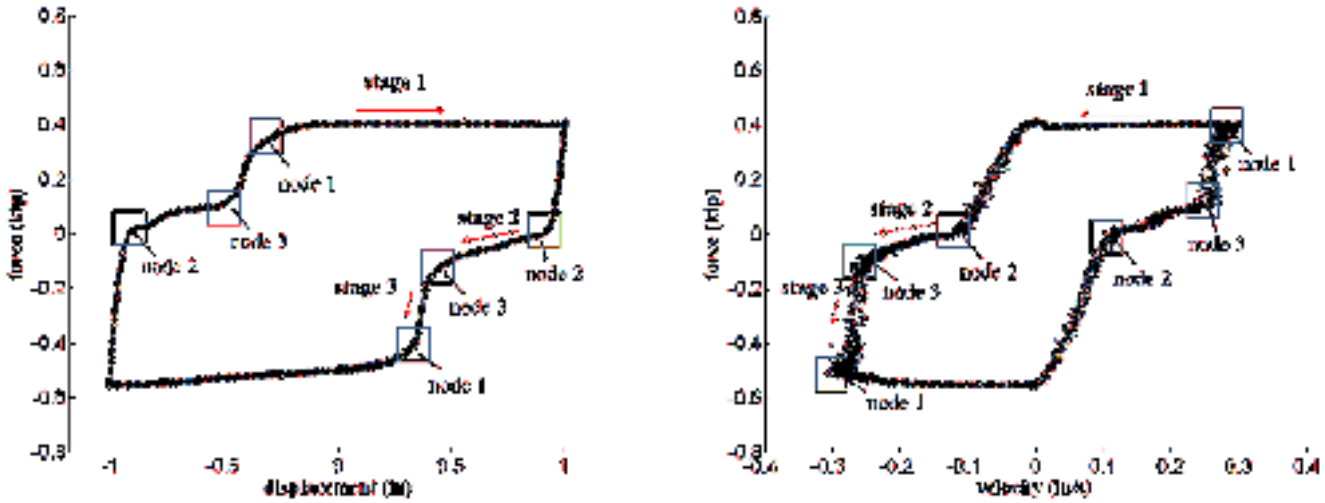

(a) (b)

Fig. 3: Dynamic response of the MFD under hydraulic pressure of 1200 psi: (a) force-displacement plot (0.05Hz); and (b) force-velocity plot (0.05Hz).

Note that d_2 can be modified (and almost eliminated) by change the design of the shoes themselves. A smooth transition region between stages is provided by a C^∞ function of the type [35]:

$$m(x) = \frac{1}{1 + e^{-\frac{\gamma_1 (x - x_0)}{\gamma_2}}} \tag{1}$$

where x_0 is the location of the new stage, and γ_1, γ_2 are constants. Consider the transition from stage i to stage j. The total force F is given by

$$F = (1 - m(x))F_i + m(x)F_j \tag{2}$$

A. LuGre Model

The LuGre model [28] is a dynamic friction model often used in the literature due to its capability to model various friction phenomena, including the Stribeck effect [29]–[33]. Using the LuGre model, the friction force during the first stage F_1 is written as follows:

$$\begin{aligned} F_1 &= \sigma_0 z + \sigma_1 \dot{z} + \sigma_2 \dot{x} \\ \dot{z} &= \dot{x} - \sigma_0 \frac{|\dot{x}|}{g(\dot{x})} z \end{aligned} \tag{3}$$

where σ_0 represents the aggregate bristle stiffness, σ_1 microdamping, σ_2 viscous friction, z an evolutionary variable, x and $\dot{x}$ the displacement and velocity, respectively, and $g(\dot{x})$ a function that describes the Stribeck effect:

$$g(\dot{x}) = F_\mathrm{c} + (F_\mathrm{s} - F_\mathrm{c}) e^{-\left(\frac{\dot{x}}{\dot{x}_\mathrm{s}}\right)^2} \tag{4}$$

where $\dot{x}_{\mathrm{s}}$ is a constant modeling the Stribeck velocity, F_{s} the static frictional force, and F_{c} the kinetic friction force. Due to the surface irregularities, friction coefficients are different between forward and backward rotations, as evidenced in Fig. 3 by the difference in the maximum positive and negative frictional forces. F_s and F_c are allowed to take two different values whether the brake rotates forward ($F_{s,fwd}$ and $F_{c,fwd}$) or backward ($F_{c,bwd}$ and $F_{c,bwd}$).

The full dynamic model contains thirteen parameters to be identified: σ_0, σ_1, σ_2, $F_{s,fwd}$, $F_{c,fwd}$, $F_{c,bwd}$, $F_{c,bwd}$, k_2, k_3, d_2, d_3, γ_1, and γ_2. Some of these parameters (F_c, F_s, σ_0) are pressure-dependent.

IV. LABORATORY EXPERIMENT

A. Methodology

To verify the proposed three-stage dynamic model, the MFD prototype has been subjected to different harmonic excitations under various pressures. The prototype was installed in an MTS testing system and subjected to a uni-axial displacement. Harmonic excitations of 1 inch amplitudes were used at 0.05 and 0.5 Hz. Five different pressures on the pneumatic actuator were tested: 0, 500, 800, 1200, and 1500 psi, where 1500 corresponds to the actuator's maximum allowable pressure. Force and displacement data were recorded by the MTS data acquisition system at a sampling rate of 100 Hz.

B. Model Parameters Optimization

Model parameters were optimized for each of the individual tests performed on the MFD. Table I lists the obtained values.

TABLE I: Individual model parameters

	0.05 Hz				0.5 Hz			
	500 psi	800 psi	1200 psi	1500psi	500 psi	800 psi	1200 psi	1500psi
σ_0 $(kip \cdot in^{-1})$	4.054	4.754	5.054	6.254	4.054	4.754	5.054	6.254
σ_1 $(psi \cdot s \cdot in^{-1})$	1.000	1.000	1.000	1.000	1.000	1.000	1.000	1.000
σ_2 $(psi \cdot s \cdot in^{-1})$	1.000	1.000	1.000	1.000	1.000	1.000	1.000	1.000
$F_{\mathrm{c,fwd}}(kip)$	0.142	0.239	0.403	0.530	0.143	0.260	0.412	0.536
$F_{\mathrm{c,bwd}}(kip)$	-0.181	-0.295	-0.549	-0.710	-0.183	-0.340	-0.587	-0.710
$F_{\mathrm{s,fwd}}(kip)$	0.152	0.251	0.417	0.549	0.155	0.269	0.417	0.538
$F_{\mathrm{s,bwd}}(kip)$	-0.185	-0.305	-0.563	-0.727	-0.188	-0.341	-0.595	-0.730
k_2 $(kip \cdot in^{-1})$	0.231	0.231	0.231	0.231	0.231	0.231	0.231	0.231
k_3 $(kip \cdot in^{-1})$	3.000	3.000	3.000	3.000	3.000	3.000	3.000	3.000
$d_2(in)$	0.500	0.500	0.500	0.500	0.500	0.500	0.500	0.500
$d_3(in)$	0.200	0.200	0.200	0.200	0.200	0.200	0.200	0.200
γ_1	1.000	1.000	1.000	1.000	1.000	1.000	1.000	1.000
$\gamma_2(in)$	0.100	0.100	0.100	0.100	0.100	0.100	0.100	0.100

Results from Table I shows that the model parameters can be estimated as independent on excitation frequencies, but vary linearly with respect to actuation force p (pressure) in the form:

$$\begin{aligned} \sigma_0 &= \alpha_{\sigma_0} p + \sigma_0|_{p=0} \\ F_{\mathrm{c,fwd}} &= K_{\mathrm{c,fwd}} p \\ f_{\mathrm{c,bwd}} &= K_{\mathrm{c,bwd}} p \\ F_{\mathrm{s,fwd}} &= K_{\mathrm{s,fwd}} p \\ F_{\mathrm{s,bwd}} &= K_{\mathrm{s,bwd}} p \end{aligned} \tag{5}$$

where α_{σ_0} is constant, and $\sigma_0|_{p=0}$ denotes the base value for σ_0 at $p = 0\ kip \cdot in^{-2}$. Table II lists the values of these parameters computed using least square estimators.

C. Experimental versus Numerical Results

Figs. 4 to 7 show typical plots of experimental versus numerical values using the 3-stage dynamic model. Results show that the proposed dynamic model provides a good approximation of experimental data.

TABLE II: Parameters for pressure-dependant variables

Parameter	Value
$\alpha_{\sigma_0}(in)$	2×10^{-3}
$\sigma_0\|_{P=0}(kip\cdot in^{-1})$	3.029
$K_{\text{c,up}}(kip\cdot in^{-2})$	0.341
$K_{\text{c,down}}(kip\cdot in^{-2})$	0.457
$K_{\text{s,up}}(kip\cdot in^{-2})$	0.350
$K_{\text{s,down}}(kip\cdot in^{-2})$	0.467

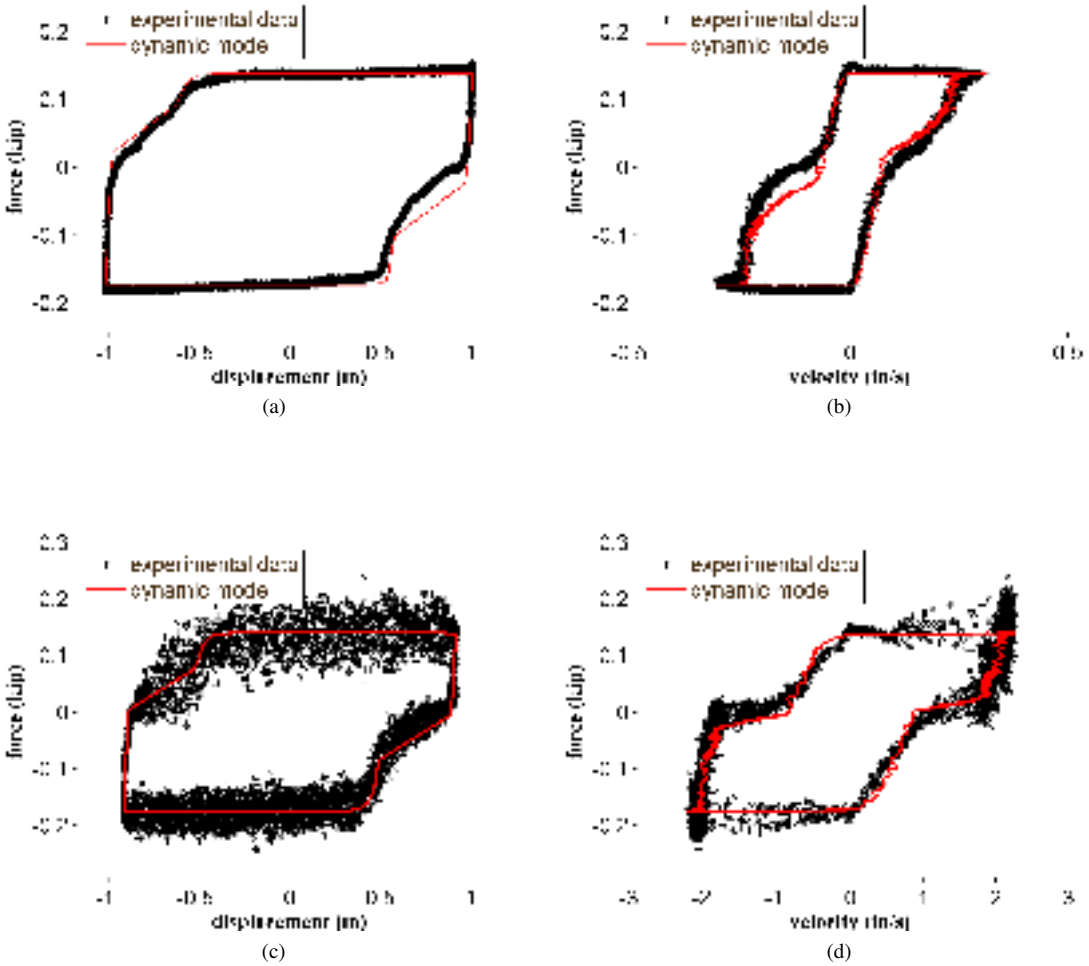

(a) (b) (c) (d)

Fig. 4: Model fitting of the MFD under 500 psi: (a) force-displacement (0.05Hz); (b) force-velocity (0.05Hz); (c) force-displacement (0.5Hz); (d) force-velocity (0.5Hz)

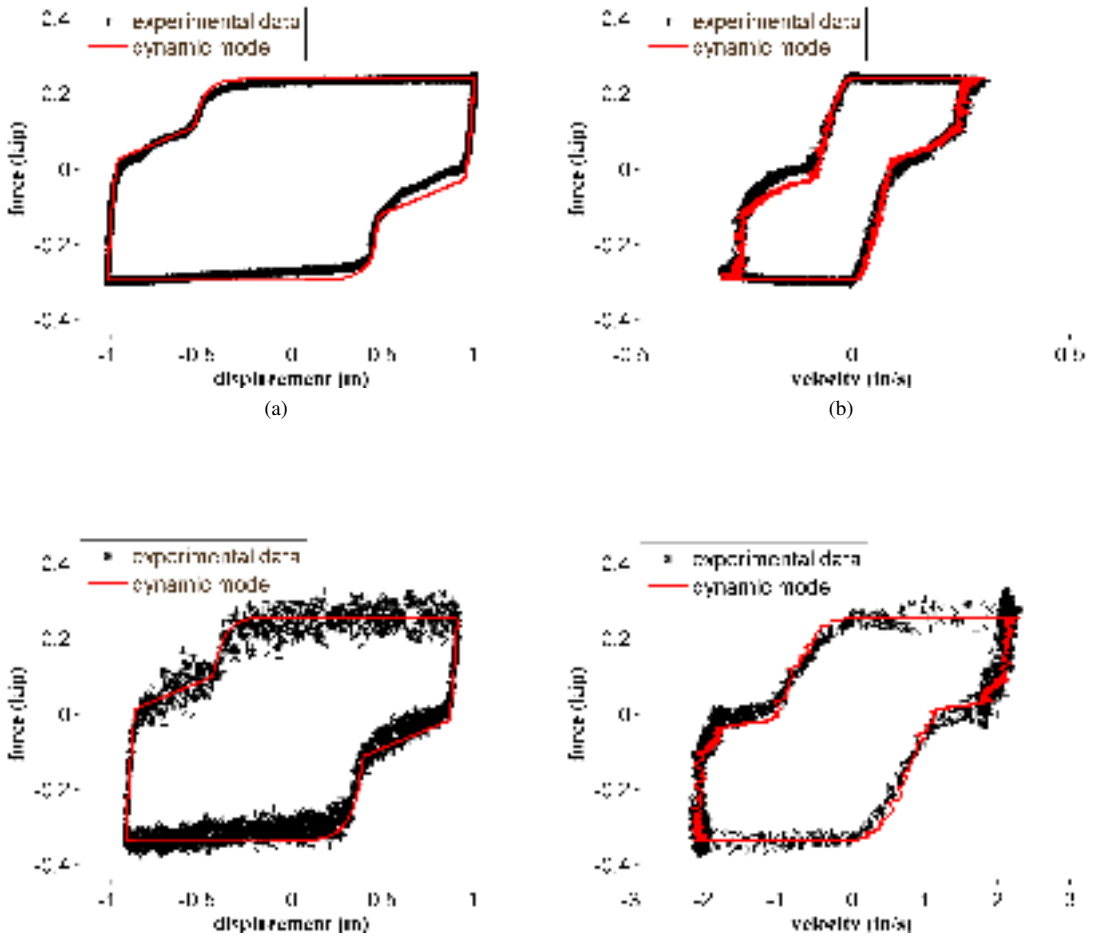

(a) (b) (c) (d)

Fig. 5: Model fitting of the MFD under 800 psi: (a) force-displacement (0.05Hz); (b) force-velocity (0.05Hz); (c) force-displacement (0.5Hz); (d) force-velocity (0.5Hz)

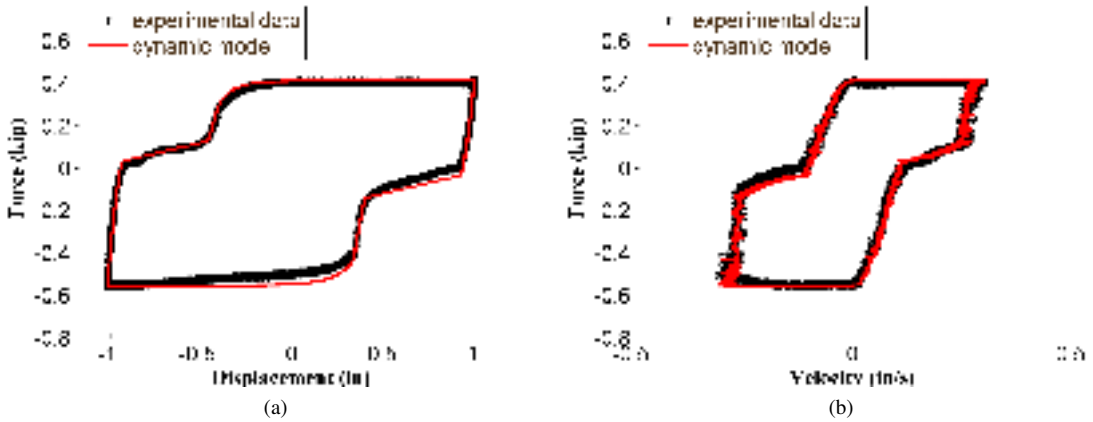

(a) (b)

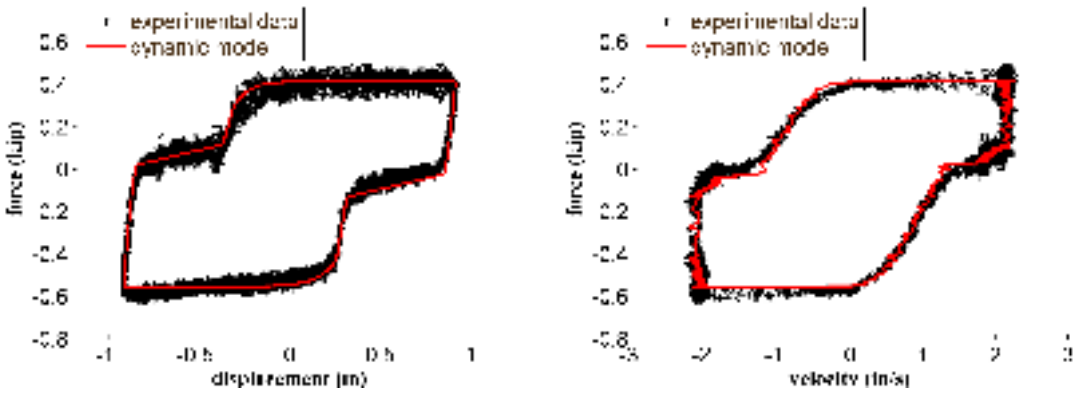

(c) (d)

Fig. 6: Model fitting of the MFD under 1200 psi: (a) force-displacement (0.05Hz); (b) force-velocity (0.05Hz); (c) force-displacement (0.5Hz); (d) force-velocity (0.5Hz)

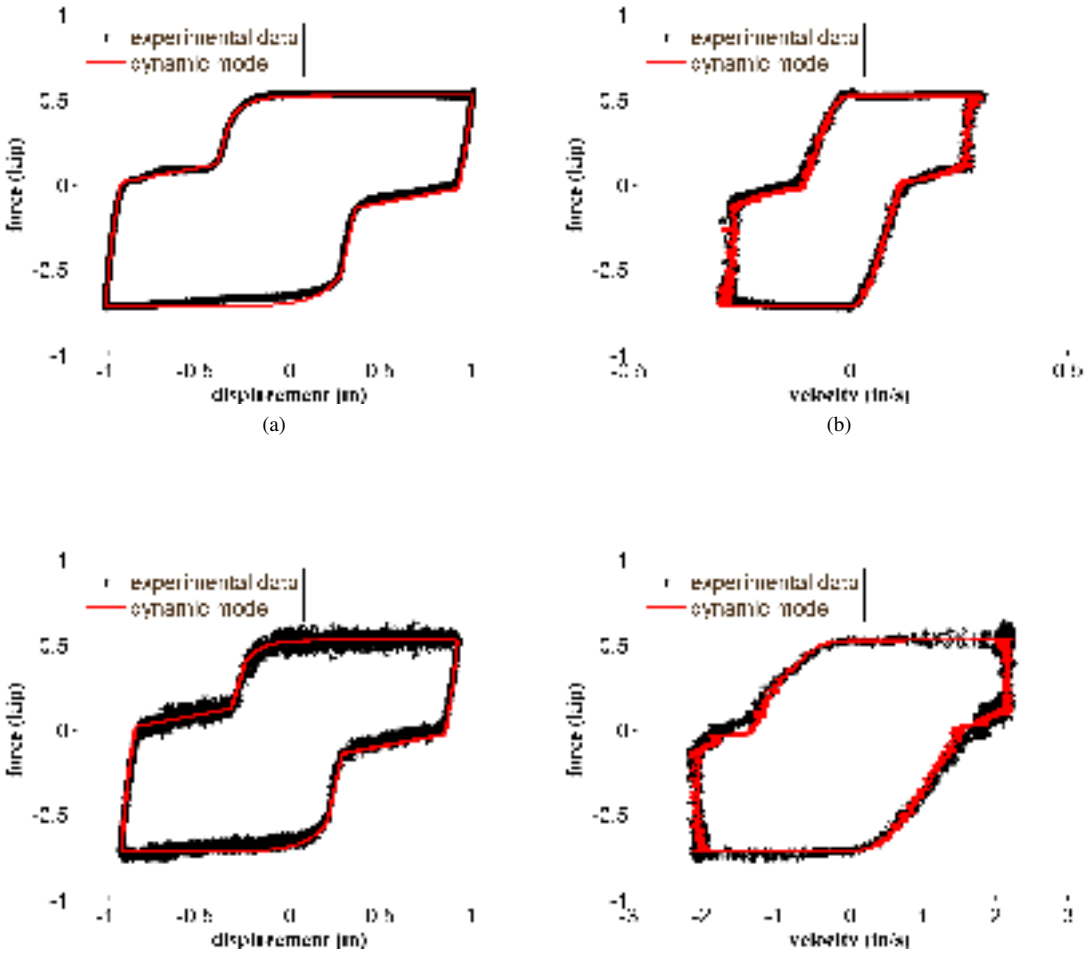

(a) (b)

(c) (d)

Fig. 7: Model fitting of the MFD under 1500 psi: (a) force-displacement (0.05Hz); (b) force-velocity (0.05Hz); (c) force-displacement (0.5Hz); (d) force-velocity (0.5Hz)

V. SUMMARY AND CONCLUSIONS

A 3-stage dynamic models has been presented to characterize the dynamic behavior of the MFD, a variable friction device. Stage 1 models the friction using the LuGre model; stage 2 models a linear stiffness found in the system when the direction is reversed, and stage 3 models the rapid build up of forces linearly. Both Stages 2 and 3 are characterized using stiffness elements. A smooth transition between dynamic stages is ensured by a sigmoid function.

Experimental results show that the model can be used under different pressures (force input) using a linear dependence of LuGre parameters on the pressure input. Numerical results show that the model provides a good fit to all experimental results under various frequencies (0.05 and 0.5 Hz) and pressures (500, 800, 1200, and 1500 psi).

The proposed dynamic model furthers the understanding of the MFD for applications to structural control. Future work on the characterization of the MFD's dynamic will include a broader range of frequencies, various displacements, and time-varying force inputs.

ACKNOWLEDGMENTS

This work is supported by Grant No.1300960 from the National Science Foundation. Their support is gratefully acknowledged. The opinions and conclusions expressed in this paper are those of the authors and not the sponsor.

REFERENCES

[1] Agrawal, Anil K., and Jann N. Yang. "Semiactive control strategies for buildings subject to near-field earthquakes." SPIE's 7th Annual International Symposium on Smart Structures and Materials. International Society for Optics and Photonics, 2000..
[2] Yang, Jann N., and Anil K. Agrawal. "Semi-active hybrid control systems for nonlinear buildings against near-field earthquakes." Engineering Structures 24.3 (2002): 271-280.
[3] He, W. L., A. K. Agrawal, and J. N. Yang. "Novel semiactive friction controller for linear structures against earthquakes." Journal of Structural Engineering 129.7 (2003): 941-950.
[4] Wongprasert, N., and M. D. Symans. "Numerical evaluation of adaptive base-isolated structures subjected to earthquake ground motions." Journal of engineering mechanics 131.2 (2005): 109-119.
[5] Liu, Yanqing, Hiroshi Matsuhisa, and Hideo Utsuno. "Semi-active vibration isolation system with variable stiffness and damping control." Journal of sound and vibration 313.1 (2008): 16-28
[6] Yang, Jann N., Jin-H. Kim, and Anil K. Agrawal. "Resetting semiactive stiffness damper for seismic response control." Journal of Structural Engineering 126.12 (2000): 1427-1433.
[7] Li, Hong-Nan, and Da-Hai Zhao. "Control of structure with semi-active friction damper by intelligent algorithm." Fuzzy Systems, 2006 IEEE International Conference on. IEEE, 2006.
[8] Yan, An Zhi, Qi Kong, and Jing Jing Lu. "Research on Control Effectiveness of Semi-Active MR-TMD to some Coal Gas Manufacturing Plant." Applied Mechanics and Materials 117 (2012): 3-8.
[9] Yang, Guangqiang, et al. "Dynamic modeling of large-scale magnetorheological damper systems for civil engineering applications." Journal of Engineering Mechanics 130.9 (2004): 1107-1114.
[10] Yoshida, Osamu, and Shirley J. Dyke. "Seismic control of a nonlinear benchmark building using smart dampers." Journal of engineering mechanics 130.4 (2004): 386-392.
[11] Yang, J. N., et al. "Full scale experimental verification of resetable semi-active stiffness dampers." Earthquake engineering and structural dynamics 36.9 (2007): 1255-1273.
[12] Cao L., Downey A., Laflamme S., Taylor D. and Ricles J., (2014). "A Novel Variable Friction Device for Natural Hazard Mitigation". In Proc. Tenth U.S. National Conference on Earthquake Engineering.
[13] Rao, S. S., and Lingtao Cao. "Optimum design of mechanical systems involving interval parameters." Journal of Mechanical Design 124.3 (2002): 465-472.
[14] Laflamme, Simon, et al. "Modified friction device for control of largescale systems." Structural control and health monitoring 19.4 (2012): 548-564.
[15] Eriksson, Mikael, John Lord, and Staffan Jacobson. "Wear and contact conditions of brake pads: dynamical in situ studies of pad on glass." Wear 249.3 (2001): 272-278.
[16] Dyke, S. J., et al. "An experimental study of MR dampers for seismic protection." Smart materials and structures 7.5 (1998): 693.
[17] Olsson, Henrik, et al. "Friction models and friction compensation." European journal of control 4.3 (1998): 176-195.
[18] Dowson, Duncan, and Duncan Dowson. History of tribology. London: Longman, 1979.
[19] Christopoulos, Constantin, Andr Filiatrault, and Vitelmo Victorio Bertero. Principles of passive supplemental damping and seismic isolation. IUSS Press, 2006.
[20] Blau, Peter J. "The significance and use of the friction coefficient." Tribology International 34.9 (2001): 585-591.
[21] Lu, Xiaobin, M. M. Khonsari, and E. R. M. Gelinck. "The Stribeck curve: experimental results and theoretical prediction." Journal of tribology 128.4 (2006): 789-794.
[22] Karnopp, Dean. "Computer simulation of stick-slip friction in mechanical dynamic systems." Trans. ASME, J. Dyn. Syst. Meas. Control 107 (1985): 100-103.
[23] Armstrong-Hlouvry, Brian, Pierre Dupont, and Carlos Canudas De Wit. "A survey of models, analysis tools and compensation methods for the control of machines with friction." Automatica 30.7 (1994): 1083-1138.
[24] Dahl, Philip R. "Solid friction damping of mechanical vibrations." AIAA Journal 14.12 (1976): 1675-1682.
[25] Valanis, K. C. A theory of viscoplasticity without a yield surface. Part 1. General theory. IOWA UNIV IOWA CITY DEPT OF MECHANICS AND HYDRAULICS, 1970.
[26] Gaul, L., and R. Nitsche. "The role of friction in mechanical joints." Applied Mechanics Reviews 54 (2001): 93.
[27] Haessig Jr, David A., and Bernard Friedland. "Modeling and simulation of friction." Orlando'91, Orlando, FL. International Society for Optics and Photonics, 1991.
[28] Canudas de Wit, Carlos, et al. "A new model for control of systems with friction." Automatic Control, IEEE Transactions on 40.3 (1995): 419-425.
[29] Altpeter, Friedhelm. Friction modeling, identification and compensation. Diss. COLE POLYTECHNIQUE FDRALE DE LAUSANNE, 1999.
[30] De Wit, C. Canudas, and Pablo Lischinsky. "Adaptive friction compensation with partially known dynamic friction model." International journal of adaptive control and signal processing 11.1 (1997): 65-80.

[31] Shiriaev, Anton, Anders Robertsson, and Rolf Johansson. "Friction compensation for passive systems based on the LuGre model." Lagrangian and Hamiltonian Methods for Nonlinear Control 2003: A Proceedings Volume from the 2nd IFAC Workshop, Seville, Spain, 3-5 April, 2003. Access Online via Elsevier, 2003.
[32] Lischinsky, P., C. Canudas-de-Wit, and G. Morel. "Friction compensation for an industrial hydraulic robot." Control Systems, IEEE 19.1 (1999): 25-32.
[33] Jimnez, Ren, and Luis lvarez Icaza. "LuGre friction model for a magnetorheological damper." Structural Control and Health Monitoring 12.1 (2005): 91-116.
[34] Johanastrom, K., and Carlos Canudas-De-Wit. "Revisiting the LuGre friction model." Control Systems, IEEE 28.6 (2008): 101-114.
[35] Laflamme, S., J. J. E. Slotine, and J. J. Connor. "Wavelet network for semi-active control." Journal of Engineering Mechanics 137.7 (2011): 462-474.